

Article

Latently activated granulocytes from an autoimmune uveitis model show divergent pathway activation profiles upon IL8 stimulation *in vitro*

Anne L.C. Hoffmann¹, Stefanie M. Hauck², Cornelia A. Deeg¹ and Roxane L. Degroote^{1,*}

¹ Chair of Physiology, Department of Veterinary Sciences, LMU Munich, D-82152 Martinsried, Germany; anne.hoffmann@tiph.vetmed.uni-muenchen.de (A.H.); cornelia.deeg@lmu.de (C.D.)

² Research Unit Protein Science, Helmholtz Center Munich, German Research Center for Environmental Health, D-80939 Munich, Germany; hauck@helmholtz-muenchen.de

* Correspondence: r.degroote@lmu.de

Abstract: In the pathophysiology of autoimmune-mediated uveitis, granulocytes have emerged as possible disease mediators and were shown to be latently activated in equine recurrent uveitis (ERU), a spontaneous disease model. We therefore used granulocytes from ERU horses to identify early molecular mechanisms involved in this dysregulated innate immune response. Primary granulocytes from healthy and ERU horses were stimulated with IL8 and cellular response was analyzed with differential proteomics, which revealed significant differences in protein abundance of 170 proteins in ERU. Subsequent ingenuity pathway analysis identified three activated canonical pathways “PKA signaling”, “PTEN signaling” and “leukocyte extravasation”. Clustered to the leukocyte extravasation pathway, we found the membrane-type GPI-anchored protease MMP25, which was increased in IL8 stimulated ERU granulocytes. These findings point to MMP25 as a possible regulator of granulocyte extravasation in uveitis and a role of this molecule in the impaired integrity of the blood-retina-barrier. In conclusion, our analyses show a clearly divergent reaction profile of latently activated granulocytes upon IL8 stimulation, and provide basic information for further in-depth studies on early granulocyte activation in non-infectious ocular diseases. This may be of interest for development of new approaches in uveitis diagnostics and therapy. Raw data are available via ProteomeXchange with identifier PXD013648.

Keywords: ERU; IL8; PMN; granulocyte; latent activation; extravasation.

1. Introduction

Understanding the molecular mechanisms involved in divergent immune response in autoimmune uveitis is indispensable for deeper insights into disease pathogenesis, which in consequence may contribute to new approaches in diagnostics and therapy. Although a dysregulated T cell response is widely recognized as a key driver in disease pathogenesis, involvement of innate immune cells has also become evident [1,2]. Early ocular influx of granulocytes was described in rodent models of experimental autoimmune uveitis [1,3-7] and has also been observed in ERU horses [8]. However, the specific role of these cells in onset and relapsing of disease is not completely understood so far.

Equine recurrent Uveitis (ERU) is a spontaneously occurring, remitting-relapsing painful disease and a leading cause of blindness among horses worldwide [9,10]. Besides its importance for veterinary medicine, it is also a valuable spontaneous model for autoimmune uveitis due to strong clinical and pathological similarities [11,12]. Concordant to autoimmune uveitis, ERU is demonstrably T-cell driven, but ocular infiltration of granulocytes has also been observed [8]. Previously, we could show that granulocytes change their protein abundance repertoire in ERU, suggesting a role of these cells in disease pathogenesis through integrin signaling, MHCII cross presentation and impairment of the blood-retinal-barrier, all of which point to a latently preactivated phenotype in disease

[13-15]. Since we were especially interested in the behavior of these latently preactivated granulocytes in an inflammatory environment, we now analyzed their reaction profile to stimulation IL8, a potent and specific chemoattractant for granulocytes [16]. With these studies, we aim at gaining more insight into the early molecular mechanisms involved in dysregulated innate immune response in uveitis and the role of granulocytes in T-cell mediated ocular disease.

2. Results

2.1. Short stimulation with IL8 shows divergent reaction profile in granulocytes from horses with recurrent uveitis.

With differential proteomics, we identified 2012 proteins in equine granulocytes (Figure 1, Table S1). Comparison of the proteomes of IL8-stimulated granulocytes revealed 170 proteins with significantly altered abundance between healthy controls and ERU cases (Table S1). Of these differentially expressed proteins, 126 were lower abundant and 44 were higher abundant in granulocytes of horses with ERU (Figure 1).

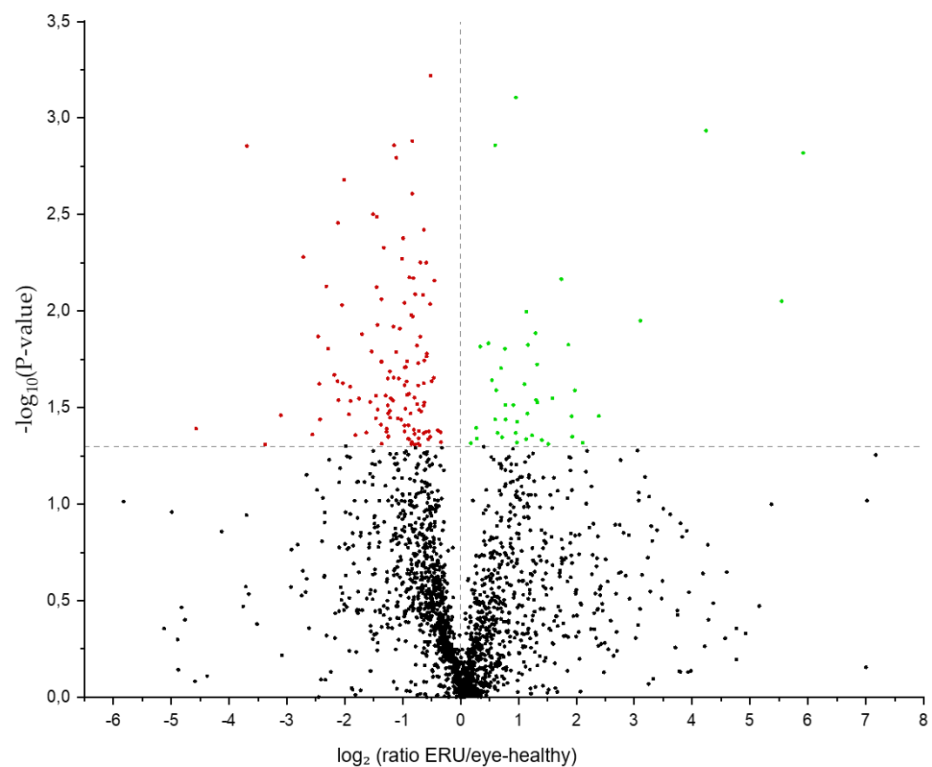


Figure 1. Volcano plot of the 2012 proteins detected by mass spectrometry. The 170 differentially abundant candidates ($p < 0.05$) between controls and ERU cases are displayed above the grey line. Higher abundant proteins are displayed in green, lower abundant proteins are marked red.

2.2. Canonical pathways Protein Kinase A Signaling, PTEN Signaling and Leukocyte Extravasation are activated in granulocytes of ERU horses.

For interpretation of the detected protein abundance differences in a broader biological context, we subjected our dataset to ingenuity pathway analysis (IPA; Qiagen, Hilden, Germany), which revealed a total of 76 significantly enriched canonical pathways (Table S2). While 57 of these pathways either did not show a changed activity pattern between groups or did not allow activity pattern prediction (Table S2), we detected 16 canonical pathways, which were inhibited in ERU samples (Figure 2, Table S2). Among these, strongest activation was predicted for “phosphatidylinositol 3-kinase/Aktin (PI3K/Akt) Signaling” (Figure 2, Table S2). In contrast, the three pathways “Protein Kinase A (PKA) Signal-

ing”, “Phosphatase and tensin homologue (PTEN) Signaling” and “Leukocyte Extravasation” showed a clear activation in IL8 stimulated granulocytes from ERU cases compared to eye-healthy controls (Figure 2, Figure 3, Table S2).

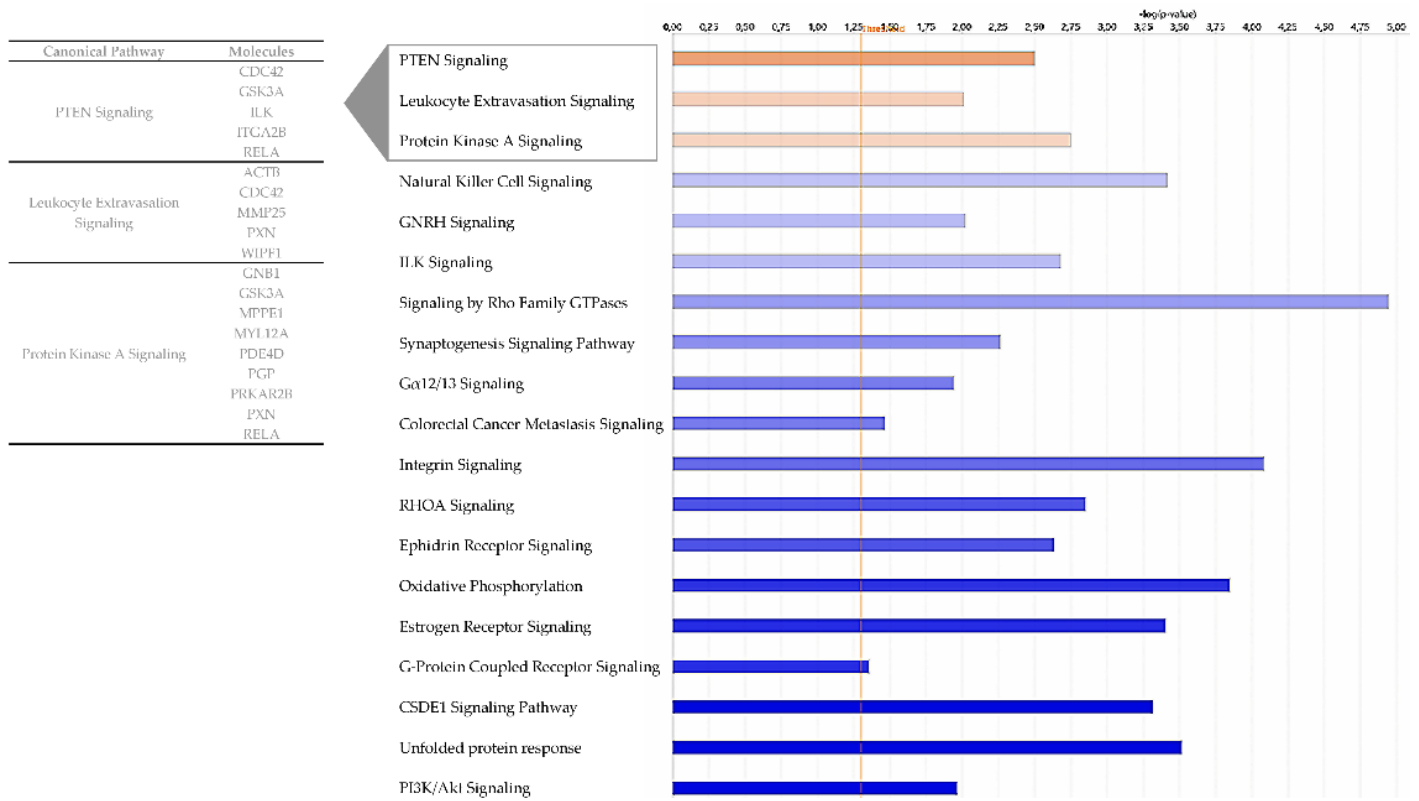


Figure 2. Bar chart showing all enriched pathways with a positive (orange) or negative (blue) z-score for prediction of activation in Ingenuity Pathway Analysis. Color intensity correlates with z-score, while bar length indicates statistical significance. The yellow line represents the p-value threshold. Gene names of differentially abundant proteins from our input dataset ($p < 0.05$) associating to the three activated pathways are shown.

2.3. Activated pathways in ERU associate to processes in cell motility and migration

All activated pathways identified with IPA associated to processes in cell motility and migration. This is reflected in the proteins allocated to these pathways, which are mainly associated to cytoskeleton organization, cell adhesion and cell migration. In detail, nine differentially expressed proteins from our dataset clustered to Protein Kinase A (PKA) Signaling: G protein subunit beta 1 (GNB1), glycogen synthase kinase 3 alpha (GSK3A), metallophosphoesterase 1 (MPPE1), myosin light chain 12A (MYL12A), phosphodiesterase 4D (PDE4D), phosphoglycolate phosphatase (PGP), protein kinase cAMP-dependent type II regulatory subunit beta (PRKAR2B), paxillin (PXN) and RELA proto-oncogene, NF- κ B subunit (RELA) (Table S2, Figure 2). Five proteins were allocated to the PTEN Signaling pathway, namely cell division cycle 42 (CDC42), glycogen synthase kinase 3 alpha (GSK3A), integrin linked kinase (ILK), integrin subunit alpha 2b (ITGA2B) and RELA proto-oncogene, NF- κ B subunit (RELA) (Table S2, Figure 2).

Since leukocyte extravasation is a crucial step in the pathogenesis of ERU, we were especially interested in the proteins allocated to this pathway (Table S2, Figure 2). Five proteins from our dataset were mapped to this pathway, of which four were associated to actin cytoskeleton organisation and signaling, namely actin beta (ACTB) and cell division cycle 42 (CDC42) (both upregulated in ERU) as well as paxillin (PXN) and “WASWASL interacting protein family member 1” (WIPF1) (both downregulated in ERU) (Table S1). The fifth protein allocated to the leukocyte extravasation pathway was the plasma membrane bound matrix metalloproteinase 25 (MMP25), which showed the highest fold change among all of the five allocated proteins (2.5 fold, Figure 2, Table S1).

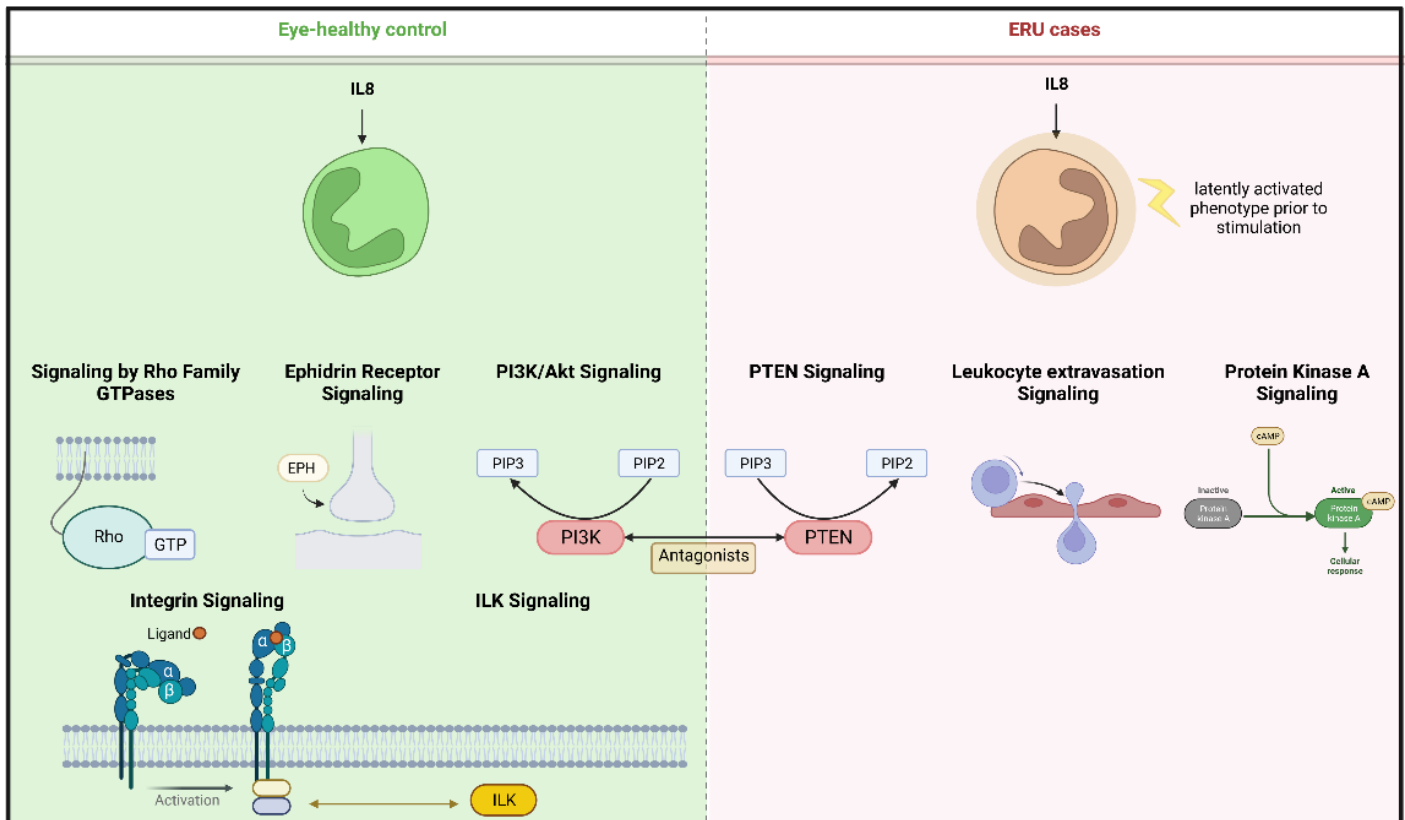


Figure 3. Overview of pathways with predicted activation after IL8 stimulation of equine granulocytes. Left panel shows canonical pathways activated in granulocytes from healthy horses; for better clarity, pathways from the same functional category were merged. Right panel shows respective activation in latently preactivated ERU granulocytes. Created with BioRender.com

3. Discussion

The participation of granulocytes in non-infectious uveitis pathogenesis has been shown in rodent uveitis models [1-3,6]. However, the exact role of these cells and their timing in and impact on ERU pathogenesis, has not been completely understood to date. On the one hand, transmigration of granulocytes over the BRB into the eye may occur as a secondary phenomenon caused by cytokine release from infiltrated lymphocytes. On the other hand, early influx of granulocytes might be an initiating factor for autoreactive behavior of adaptive immune cells. We could previously show that in a spontaneous recurrent uveitis model, granulocytes display an activated phenotype per se, even between uveitic attacks in quiescent stage of disease [15], which points to the possibility of an active rather than a bystander role in disease pathogenesis. In this study, we now detected a distinct pattern of differentially regulated proteins and associated pathways in IL8 stimulated granulocytes of ERU cases, which shows that the latently preactivated granulocytes in ERU horses react differently than their healthy counterpart.

IL8 is a chemokine, which induces chemotaxis and NETosis in primary human granulocytes [17]. Therefore, we also expected to find proteins associated to these functions in horse granulocytes. In this context, we were especially interested in the response patterns of the latently activated granulocytes from ERU horses. We identified distinct differences in pathway activation as reaction to IL8 stimulation between granulocytes from healthy horses and ERU cases (Figure 2, Figure 3, Table S2). Among the inhibited pathways in ERU granulocytes, we identified the PI3K/Akt signaling pathway (Figure 2, Figure 3, Table S2), which is involved in neutrophil cytoskeleton dynamics [18,19]. Inhibition of PI3K/Akt signaling pathway in human and mouse neutrophils could show that although it plays a role in polarization and movement of these cells, it is not a major player in signal generation for directed movement [18]. The inhibition of this

pathway in stimulated ERU granulocytes may therefore point to downstream suppression of random chemokinesis in favor of directional chemotaxis. This is supported by the activation of PKA-, PTEN- and leukocyte extravasation signaling pathways in these cells, which are associated to migration and chemotaxis, thus directed movement [20-22](Figure 2, Figure 3, Table S2). The role of activated PKA signaling in equine granulocytes has not been investigated in the context of autoimmune uveitis so far, however, the majority of studies on human or rodent neutrophils report a complex regulatory mechanism of this pathway in immune cell function [reviewed in [23]]. PTEN, which was also activated in ERU granulocytes (Figure 2, Figure 3, Table S2), catalyzes the dephosphorylation of phosphoinositol-(3,4,5)-triphosphat (PIP3) to phosphoinositol-(4,5)-diphosphat (PIP2) and is therefore a direct antagonist of PI3K, which phosphorylates PIP2 to PIP3 [reviewed in [24]]. Interestingly, in our analysis, PI3K/Akt signaling was among the inhibited pathways in IL8 stimulated ERU granulocytes, while the PTEN signaling pathway was activated, reflecting this reverse effect. To our knowledge we are the first to describe an activated PTEN Signaling in ERU, though it is convenient with our results in previous studies, showing that the PI3K Signaling is activated in granulocytes of eye-healthy controls after IL8 stimulation [16]. Overexpression of PTEN was linked to an increased NET formation in human promyelocytic leukemia (HL-60) differentiated neutrophil-like cells [25], a process which is also more readily activated in neutrophils of ERU horses [26]. Although PTEN signaling serves complex functions in neutrophil chemotaxis, cell motility and polarity [[21], reviewed in [24]], association with autoimmunity and autoimmune disease is mainly through inhibition of this pathway [27-29]. Most of the studies describing the involvement of PTEN in autoimmunity mainly focus on T- or B-cells [30], while the role of PTEN signaling in neutrophils in terms of autoimmunity is poorly examined so far. To get a deeper insight in the function of PTEN signaling in granulocytes and its association to recurrent autoimmune uveitis, further studies are necessary.

When immune cells are activated in the periphery and leave the bloodstream to migrate into the eye, they cause damage to intraocular structures [31-33]. There are several theories on how peripheral immune cells manage to overcome the blood-retina-barrier (BRB), which is designed to maintain ocular immune privilege. For example, loss of barrier integrity might originate in the cells forming the barrier itself. On the other hand, it may occur as a secondary effect in response to recruitment of peripheral immune cells. Whatever the cause, actin cytoskeleton dynamics is a key player driving these mechanisms and a prerequisite for leukocyte extravasation [34]. Therefore, the activation of proteins of the "leukocyte extravasation pathway" in our analysis of ERU granulocytes after IL8 stimulation is interesting and points to significant changes in the cellular function of granulocytes in ERU. Since said pathway was specifically activated in ERU granulocytes (Figure 2, Figure 3, Table S2), this might point to differences needed for successful migration over the BRB. Matrix Metalloproteinase 25 (MMP25) was among the changed proteins in ERU granulocytes clustering to this pathway (Figure 2/Table S2). MMP25 is a membrane-type GPI anchored protease, which belongs to the matrix-metalloproteinase family [35,36] and plays a role in extracellular matrix remodeling and proteolysis, as well as inflammatory responses such as trans-endothelial migration of neutrophils to inflammatory sites [37,38]. Other MMPs have previously been associated to ERU pathogenesis through changed expression levels in the equine retina and in infiltrated Th1 cells [39], however, MMP25 has not been investigated in autoimmune uveitis so far. In other autoimmune-mediated diseases it has been described as a promising drug target due to its role in activated proteolytic pathways [40]. Moreover, MMPs compromise blood-brain-barrier integrity through proteolysis of basement membrane and tight junction proteins in autoimmune-mediated disorders such as multiple sclerosis, allowing infiltration of peripheral immune cells [41,42]. The increased abundance of MMP25 in our dataset might therefore indicate a similar effect on the BRB in uveitis.

In summary, our differential proteome analyses showed, that naturally preactivated granulocytes from ERU cases exhibit an aberrant response profile to *in vitro* stimulation with the chemokine IL8. The latent activation status of these cells in ERU may therefore

promote immune dysregulation *in vivo*, suggesting an active role in autoimmune uveitis. Because the spontaneous occurring disease in the horse is a valuable model for autoimmune uveitis in humans, these findings may serve as a basis for more in-depth studies of early granulocyte activation in noninfectious ocular diseases and provide a potential starting point for the understanding of disease pathogenesis and the interplay of granulocytes and T cells in autoimmune diseases.

4. Materials and Methods

4.1. Sample processing

Primary granulocytes from heparinized (50 I.U./ml blood, Ratiopharm, Ulm, Germany) venous whole blood of three healthy horses and three ERU cases were used in this study. The healthy horses are owned by the Equine Clinic at Ludwig-Maximilians-University Munich. Horses with ERU were patients awaiting therapeutic procedure. ERU was diagnosed by experienced clinicians from the Equine Clinic at Ludwig-Maximilians-University Munich and was based on typical clinical signs of uveitis along with a documented history of multiple episodes of inflammation of the affected eye [43]. At the time of blood withdrawal, ERU horses were in quiescent stage of disease. No experimental animals were used in this study. Collection of blood was permitted by the local authority (Regierung von Oberbayern, Permit number: ROB-55.2Vet-2532.Vet_03-17-88).

After rough sedimentation of erythrocytes, granulocytes were isolated from plasma by density gradient centrifugation (room temperature, 350 x g, 25 min, brake off) with Ficoll-Paque PLUS separating solution (density 1.077 g/ml; Cytiva Life Sciences, Freiburg, Germany). The resulting interphase, containing PBMC, was discarded, cells at the bottom of the tube were carefully washed (4°C, 400 x g, 10 min) in cold PBS (DPBS devoid of CaCl₂ and MgCl₂; Gibco / ThermoFisher Scientific, Germany) and remaining erythrocytes were removed by 30 second sodium chloride (0.2% NaCl) lysis. Isotonicity of samples was restored through addition of equal parts 1.6% NaCl. Granulocytes were then washed (4°C, 400 x g, 10 min) and resuspended in PBS with 0.2% glucose.

From each animal used in the experiment, we prepared aliquot portions of 6 x 10⁵ cells / 500µl which we stimulated with recombinant equine interleukin-8 (IL8; Kingfisher Biotec; 1ng/ml) for 30 minutes in a CO₂ incubator (37°C, 5% CO₂). Subsequent to the 30 minutes incubation, the volume of each aliquot was adjusted to 1ml by adding PBS with 0.2% Glucose. Cells were then pelleted (4°C, 2300 x g, 10 min) and stored at -20°C. Prior to mass spectrometry analysis, granulocytes were thawed and lysed in urea buffer (8M urea in 0.1M Tris/HCl pH 8.5), and protein concentration was determined with Bradford protein assay [44].

4.2. Mass spectrometric analysis

From each sample, 10µg total protein was digested with LysC and trypsin by filter-aided sample preparation (FASP) as previously described [45]. Acidified eluted peptides were analyzed in a data-dependent mode on a QExactive HF mass spectrometer (Thermo Fisher Scientific) online coupled to a Ultimate 3000 RSLC nano-HPLC (Dionex). Samples were automatically injected and loaded onto the C18 trap cartridge and after 5 min eluted and separated on the C18 analytical column (nanoEase MZ HSS T3, 100Å, 1,8 µm, 75 µm x 250 mm; Waters) by a 95 min non-linear acetonitrile gradient at a flow rate of 250 nl/min. MS spectra were recorded at a resolution of 60000 with an automatic gain control (AGC) target of 3e6 and a maximum injection time of 30 ms from 300 to 1500 m/z. From the MS scan, the 10 most abundant peptide ions were selected for fragmentation via HCD with a normalized collision energy of 27, an isolation window of 1.6 m/z, and a dynamic exclusion of 30 s. MS/MS spectra were recorded at a resolution of 15000 with a AGC target of 1e5 and a maximum injection time of 50 ms. Unassigned charges, and charges of +1 and > +8 were excluded from precursor selection.

4.3. Data processing and label-free quantification

Label-free quantitative analysis was performed using Progenesis QI software (version 2.5, Nonlinear Dynamics, Waters, Newcastle upon Tyne, U.K.) as described [46,47]. Briefly, raw MS files were imported, followed by automatic peak picking and retention time alignment and normalization of total peak intensities across all samples to minimize loading differences. All MS/MS spectra were exported from Progenesis QI software as Mascot generic files (mgf) and searched against Ensembl Horse protein database (version 3.0, <http://www.ensembl.org>) for peptide identification with Mascot (version 2.5.1). Search parameters used were 10 ppm peptide mass tolerance, 20 mmu fragment mass tolerance, one missed cleavage allowed, carbamidomethylation as fixed modification and methionine oxidation as well as deamidation of asparagine and glutamine as variable modifications. Mascot integrated decoy database search was set to a false discovery rate (FDR) of 1% when searching was performed on the concatenated mgf files with a percolator ion score cut-off of 13 and an appropriate significance threshold p . Identifications were re-imported into Progenesis QI and redundancies grouped following the rules of parsimony.

4.4. Data analysis

Differential protein abundance was determined by comparison of the mean normalized peptide abundance from the extracted ion chromatograms. Proteins abundance differences were considered significant at $p < 0.05$. Bioinformatic analysis was performed on human orthologues (rarely, on mouse orthologues, if human orthologue gene name was not available) of gene names from significant, differentially expressed equine proteins with Ingenuity Pathway Analysis (IPA; Qiagen, Hilden, Germany, <https://digitalinsights.qiagen.com/>). Z-score describes prediction of activation or inhibition of respective pathway, significance threshold was set to $-\log(p\text{-value}) > 1.3$. IPA analyses overrepresentation of proteins from data input in canonical pathways deposited in the IPA library, as previously described.[48]. This allows insight on possible physiological effects of upstream molecules on these proteins and allocation to downstream pathways. Analysis was performed based on the abundance ratio p -value of the stimulated samples. Volcano plot was visualized with OriginPro 2020 software (Additive, Friedrichsdorf, Germany).

Supplementary Materials: The following supporting information can be downloaded at: www.mdpi.com/xxx/s1, Table S1: all IDs after IL8 stimulation; Table S2: IPA analysis results.

Author Contributions: Conceptualization, R.D. and C.D.; formal analysis, S.H. and A.H.; investigation, R.D., S.H. and A.H.; resources, C.D. and S.H.; writing—original draft preparation, R.D. and A.H.; writing—review and editing, R.D., A.H., C.D. and S.H.; visualization, A.H.; supervision, R.D. and C.D.; project administration, R.D. and C.D.; funding acquisition, C.D.. All authors have read and agreed to the published version of the manuscript.

Funding: This research was funded by Deutsche Forschungsgemeinschaft, DFG DE 719/4-3 (to C.D.).

Institutional Review Board Statement: No experimental animals were used in this study. Horses were treated according to the ethical principles and guidelines in the ARVO statement for the use of animals in Ophthalmic and Vision research. Collection of blood was permitted by the local authority, Regierung von Oberbayern (Permit number: ROB-55.2Vet-2532.Vet_03-17-88, date of approval: 14.11 2017, permit effective from 30.12.2017).

Data Availability Statement: The raw mass spectrometry proteomics data have been deposited to the ProteomeXchange Consortium via the PRIDE [49] partner repository with the dataset identifier PXD013648.

Acknowledgments: The authors want to thank the staff from LMU Munich equine clinic, especially Tanja Witte and Kirsten Hahn for supplying equine blood samples, and Adrian Schmalen for critical discussions.

Conflicts of Interest: The authors declare no conflict of interest. The funders had no role in the design of the study; in the collection, analyses, or interpretation of data; in the writing of the manuscript, or in the decision to publish the results.

References

1. Kerr, E.C.; Raveney, B.J.; Copland, D.A.; Dick, A.D.; Nicholson, L.B. Analysis of retinal cellular infiltrate in experimental autoimmune uveoretinitis reveals multiple regulatory cell populations. *J Autoimmun* **2008**, *31*, 354-361, doi:10.1016/j.jaut.2008.08.006.
2. Kerr, E.C.; Copland, D.A.; Dick, A.D.; Nicholson, L.B. The dynamics of leukocyte infiltration in experimental autoimmune uveoretinitis. *Prog Retin Eye Res* **2008**, *27*, 527-535, doi:10.1016/j.preteyeres.2008.07.001.
3. Pepple, K.L.; Wilson, L.; Van Gelder, R.N. Comparison of Aqueous and Vitreous Lymphocyte Populations From Two Rat Models of Experimental Uveitis. *Invest Ophthalmol Vis Sci* **2018**, *59*, 2504-2511, doi:10.1167/iovs.18-24192.
4. Jones, L.S.; Rizzo, L.V.; Agarwal, R.K.; Tarrant, T.K.; Chan, C.C.; Wiggert, B.; Caspi, R.R. IFN-gamma-deficient mice develop experimental autoimmune uveitis in the context of a deviant effector response. *J Immunol* **1997**, *158*, 5997-6005.
5. Kim, S.J.; Zhang, M.; Vistica, B.P.; Chan, C.C.; Shen, D.F.; Wawrousek, E.F.; Gery, I. Induction of ocular inflammation by T-helper lymphocytes type 2. *Invest Ophthalmol Vis Sci* **2002**, *43*, 758-765.
6. Su, S.B.; Grajewski, R.S.; Luger, D.; Agarwal, R.K.; Silver, P.B.; Tang, J.; Tuo, J.; Chan, C.C.; Caspi, R.R. Altered chemokine profile associated with exacerbated autoimmune pathology under conditions of genetic interferon-gamma deficiency. *Invest Ophthalmol Vis Sci* **2007**, *48*, 4616-4625, doi:10.1167/iovs.07-0233.
7. Caspi, R.R.; Chan, C.C.; Fujino, Y.; Najafian, F.; Grover, S.; Hansen, C.T.; Wilder, R.L. Recruitment of antigen-nonspecific cells plays a pivotal role in the pathogenesis of a T cell-mediated organ-specific autoimmune disease, experimental autoimmune uveoretinitis. *J Neuroimmunol* **1993**, *47*, 177-188, doi:10.1016/0165-5728(93)90028-w.
8. Deeg, C.A.; Kaspers, B.; Gerhards, H.; Thurau, S.R.; Wollanke, B.; Wildner, G. Immune responses to retinal autoantigens and peptides in equine recurrent uveitis. *Invest Ophthalmol Vis Sci* **2001**, *42*, 393-398.
9. Gilger, B.C.; Michau, T.M. Equine recurrent uveitis: new methods of management. *Vet Clin North Am Equine Pract* **2004**, *20*, 417-427, vii, doi:10.1016/j.cveq.2004.04.010S0749073904000288 [pii].
10. Allbaugh, R.A. Equine recurrent uveitis: A review of clinical assessment and management. *Equine Veterinary Education* **2016**, n/a-n/a, doi:10.1111/eve.12548.
11. Malalana, F.; Stylianides, A.; McGowan, C. Equine recurrent uveitis: Human and equine perspectives. *Vet J* **2015**, *206*, 22-29, doi:10.1016/j.tvjl.2015.06.017.
12. Deeg, C.A.; Hauck, S.M.; Amann, B.; Pompetzki, D.; Altmann, F.; Raith, A.; Schmalzl, T.; Stangassinger, M.; Ueffing, M. Equine recurrent uveitis--a spontaneous horse model of uveitis. *Ophthalmic Res* **2008**, *40*, 151-153, doi:000119867 [pii] 10.1159/000119867.
13. Degroote, R.L.; Hauck, S.M.; Kremmer, E.; Amann, B.; Ueffing, M.; Deeg, C.A. Altered expression of talin 1 in peripheral immune cells points to a significant role of the innate immune system in spontaneous autoimmune uveitis. *Journal of proteomics* **2012**, *75*, 4536-4544, doi:10.1016/j.jpro.2012.01.023.
14. Degroote, R.L.; Hauck, S.M.; Treutlein, G.; Amann, B.; Frohlich, K.J.; Kremmer, E.; Merl, J.; Stangassinger, M.; Ueffing, M.; Deeg, C.A. Expression Changes and Novel Interaction Partners of Talin 1 in Effector Cells of Autoimmune Uveitis. *J Proteome Res* **2013**, doi:10.1021/pr400837f.
15. Weigand, M.; Hauck, S.M.; Deeg, C.A.; Degroote, R.L. Deviant proteome profile of equine granulocytes associates to latent activation status in organ specific autoimmune disease. *Journal of proteomics* **2020**, *230*, 103989, doi:10.1016/j.jpro.2020.103989.
16. Degroote, R.L.; Weigand, M.; Hauck, S.M.; Deeg, C.A. IL8 and PMA Trigger the Regulation of Different Biological Processes in Granulocyte Activation. *Frontiers in immunology* **2019**, *10*, 3064, doi:10.3389/fimmu.2019.03064.
17. Bernhard, S.; Hug, S.; Stratmann, A.E.P.; Erber, M.; Vidoni, L.; Knapp, C.L.; Thomass, B.D.; Fauler, M.; Nilsson, B.; Nilsson Ekdahl, K.; et al. Interleukin 8 Elicits Rapid Physiological Changes in Neutrophils That Are Altered by Inflammatory Conditions. *Journal of innate immunity* **2021**, *13*, 225-241, doi:10.1159/000514885.

18. Ferguson, G.J.; Milne, L.; Kulkarni, S.; Sasaki, T.; Walker, S.; Andrews, S.; Crabbe, T.; Finan, P.; Jones, G.; Jackson, S.; et al. PI(3)Kgamma has an important context-dependent role in neutrophil chemokinesis. *Nat Cell Biol* **2007**, *9*, 86-91, doi:10.1038/ncb1517.
19. Feng, S.; Zhou, L.; Zhang, Y.; Lu, S.; Long, M. Mechanochemical modeling of neutrophil migration based on four signaling layers, integrin dynamics, and substrate stiffness. *Biomech Model Mechanobiol* **2018**, *17*, 1611-1630, doi:10.1007/s10237-018-1047-2.
20. Jones, S.L.; Sharief, Y. Asymmetrical protein kinase A activity establishes neutrophil cytoskeletal polarity and enables chemotaxis. *J Leukoc Biol* **2005**, *78*, 248-258, doi:10.1189/jlb.0804459.
21. Li, Y.; Jin, Y.; Liu, B.; Lu, D.; Zhu, M.; Jin, Y.; McNutt, M.A.; Yin, Y. PTENalpha promotes neutrophil chemotaxis through regulation of cell deformability. *Blood* **2019**, *133*, 2079-2089, doi:10.1182/blood-2019-01-899864.
22. McMinn, P.H.; Hind, L.E.; Huttenlocher, A.; Beebe, D.J. Neutrophil trafficking on-a-chip: an in vitro, organotypic model for investigating neutrophil priming, extravasation, and migration with spatiotemporal control. *Lab Chip* **2019**, *19*, 3697-3705, doi:10.1039/c9lc00562e.
23. Howe, A.K. Regulation of actin-based cell migration by cAMP/PKA. *Biochim Biophys Acta* **2004**, *1692*, 159-174, doi:10.1016/j.bbamcr.2004.03.005.
24. Taylor, H.; Laurence, A.D.J.; Uhlig, H.H. The Role of PTEN in Innate and Adaptive Immunity. *Cold Spring Harb Perspect Med* **2019**, *9*, doi:10.1101/cshperspect.a036996.
25. Teimourian, S.; Moghanloo, E. Role of PTEN in neutrophil extracellular trap formation. *Mol Immunol* **2015**, *66*, 319-324, doi:10.1016/j.molimm.2015.03.251.
26. Fingerhut, L.; Ohnesorge, B.; von Borstel, M.; Schumski, A.; Strutzberg-Minder, K.; Morgelin, M.; Deeg, C.A.; Haagsman, H.P.; Beineke, A.; von Kockritz-Blickwede, M.; et al. Neutrophil Extracellular Traps in the Pathogenesis of Equine Recurrent Uveitis (ERU). *Cells* **2019**, *8*, doi:10.3390/cells8121528.
27. Wu, X.N.; Ye, Y.X.; Niu, J.W.; Li, Y.; Li, X.; You, X.; Chen, H.; Zhao, L.D.; Zeng, X.F.; Zhang, F.C.; et al. Defective PTEN regulation contributes to B cell hyperresponsiveness in systemic lupus erythematosus. *Sci Transl Med* **2014**, *6*, 246ra299, doi:10.1126/scitranslmed.3009131.
28. Zare-Chahoki, A.; Ahmadi-Zeidabadi, M.; Azadarmaki, S.; Ghorbani, S.; Noorbakhsh, F. Inflammation in an Animal Model of Multiple Sclerosis Leads to MicroRNA-25-3p Dysregulation Associated with Inhibition of Pten and Klf4. *Iran J Allergy Asthma Immunol* **2021**, *20*, 314-325, doi:10.18502/ijaa.v20i3.6337.
29. Bluml, S.; Sahin, E.; Saferding, V.; Goncalves-Alves, E.; Hainzl, E.; Niederreiter, B.; Hladik, A.; Lohmeyer, T.; Brunner, J.S.; Bonelli, M.; et al. Phosphatase and tensin homolog (PTEN) in antigen-presenting cells controls Th17-mediated autoimmune arthritis. *Arthritis Res Ther* **2015**, *17*, 230, doi:10.1186/s13075-015-0742-y.
30. Huynh, A.; Turka, L.A. Control of T cell tolerance by phosphatase and tensin homolog. *Ann N Y Acad Sci* **2013**, *1280*, 27-29, doi:10.1111/nyas.12015.
31. Xu, H.; Manivannan, A.; Jiang, H.R.; Liversidge, J.; Sharp, P.F.; Forrester, J.V.; Crane, I.J. Recruitment of IFN-gamma-producing (Th1-like) cells into the inflamed retina in vivo is preferentially regulated by P-selectin glycoprotein ligand 1:P/E-selectin interactions. *J Immunol* **2004**, *172*, 3215-3224, doi:10.4049/jimmunol.172.5.3215.
32. Xu, H.; Manivannan, A.; Liversidge, J.; Sharp, P.F.; Forrester, J.V.; Crane, I.J. Requirements for passage of T lymphocytes across non-inflamed retinal microvessels. *J Neuroimmunol* **2003**, *142*, 47-57.
33. Deeg, C.A.; Thurau, S.R.; Gerhards, H.; Ehrenhofer, M.; Wildner, G.; Kaspers, B. Uveitis in horses induced by interphotoreceptor retinoid-binding protein is similar to the spontaneous disease. *Eur J Immunol* **2002**, *32*, 2598-2606, doi:10.1002/1521-4141(200209)32:9<2598::AID-IMMU2598>3.0.CO;2-#.
34. Tur-Gracia, S.; Martinez-Quiles, N. Emerging functions of cytoskeletal proteins in immune diseases. *J Cell Sci* **2021**, *134*, doi:10.1242/jcs.253534.

35. Pei, D. Leukolysin/MMP25/MT6-MMP: a novel matrix metalloproteinase specifically expressed in the leukocyte lineage. *Cell research* **1999**, *9*, 291-303, doi:10.1038/sj.cr.7290028.
36. Kojima, S.; Itoh, Y.; Matsumoto, S.; Masuho, Y.; Seiki, M. Membrane-type 6 matrix metalloproteinase (MT6-MMP, MMP-25) is the second glycosyl-phosphatidyl inositol (GPI)-anchored MMP. *FEBS Lett* **2000**, *480*, 142-146, doi:10.1016/s0014-5793(00)01919-0.
37. English, W.R.; Velasco, G.; Stracke, J.O.; Knauper, V.; Murphy, G. Catalytic activities of membrane-type 6 matrix metalloproteinase (MMP25). *FEBS Lett* **2001**, *491*, 137-142, doi:10.1016/s0014-5793(01)02150-0.
38. Lerchenberger, M.; Uhl, B.; Stark, K.; Zuchtriegel, G.; Eckart, A.; Miller, M.; Pühr-Westerheide, D.; Praetner, M.; Rehberg, M.; Khandoga, A.G.; et al. Matrix metalloproteinases modulate ameoid-like migration of neutrophils through inflamed interstitial tissue. *Blood* **2013**, *122*, 770-780, doi:10.1182/blood-2012-12-472944.
39. Hofmaier, F.; Hauck, S.M.; Amann, B.; Degroote, R.L.; Deeg, C.A. Changes in matrix metalloproteinase network in a spontaneous autoimmune uveitis model. *Invest Ophthalmol Vis Sci* **2011**, *52*, 2314-2320, doi:10.1167/iovs.10-6475.
40. Shiryayev, S.A.; Remacle, A.G.; Savinov, A.Y.; Chernov, A.V.; Cieplak, P.; Radichev, I.A.; Williams, R.; Shiryayeva, T.N.; Gawlik, K.; Postnova, T.I.; et al. Inflammatory proprotein convertase-matrix metalloproteinase proteolytic pathway in antigen-presenting cells as a step to autoimmune multiple sclerosis. *J Biol Chem* **2009**, *284*, 30615-30626, doi:10.1074/jbc.M109.041244.
41. Rempe, R.G.; Hartz, A.M.S.; Bauer, B. Matrix metalloproteinases in the brain and blood-brain barrier: Versatile breakers and makers. *J Cereb Blood Flow Metab* **2016**, *36*, 1481-1507, doi:10.1177/0271678X16655551.
42. Lindberg, R.L.; De Groot, C.J.; Montagne, L.; Freitag, P.; van der Valk, P.; Kappos, L.; Leppert, D. The expression profile of matrix metalloproteinases (MMPs) and their inhibitors (TIMPs) in lesions and normal appearing white matter of multiple sclerosis. *Brain* **2001**, *124*, 1743-1753, doi:10.1093/brain/124.9.1743.
43. Werry, H.; Gerhards, H. [The surgical therapy of equine recurrent uveitis]. *Tierarztl Prax* **1992**, *20*, 178-186.
44. Bradford, M.M. A rapid and sensitive method for the quantitation of microgram quantities of protein utilizing the principle of protein-dye binding. *Anal Biochem* **1976**, *72*, 248-254, doi:10.1006/abio.1976.9999.
45. Grosche, A.; Hauser, A.; Lepper, M.F.; Mayo, R.; von Toerne, C.; Merl-Pham, J.; Hauck, S.M. The Proteome of Native Adult Muller Glial Cells From Murine Retina. *Mol Cell Proteomics* **2016**, *15*, 462-480, doi:10.1074/mcp.M115.052183.
46. Hauck, S.M.; Hofmaier, F.; Dietter, J.; Swadzba, M.E.; Blindert, M.; Amann, B.; Behler, J.; Kremmer, E.; Ueffing, M.; Deeg, C.A. Label-free LC-MSMS analysis of vitreous from autoimmune uveitis reveals a significant decrease in secreted Wnt signalling inhibitors DKK3 and SFRP2. *Journal of proteomics* **2012**, *75*, 4545-4554, doi:10.1016/j.jprot.2012.04.052.
47. Hauck, S.M.; Lepper, M.F.; Hertl, M.; Sekundo, W.; Deeg, C.A. Proteome Dynamics in Biobanked Horse Peripheral Blood Derived Lymphocytes (PBL) with Induced Autoimmune Uveitis. *Proteomics* **2017**, *17*, doi:10.1002/pmic.201700013.
48. Kramer, A.; Green, J.; Pollard, J., Jr.; Tugendreich, S. Causal analysis approaches in Ingenuity Pathway Analysis. *Bioinformatics* **2014**, *30*, 523-530, doi:10.1093/bioinformatics/btt703.
49. Perez-Riverol, Y.; Csordas, A.; Bai, J.; Bernal-Llinares, M.; Hewapathirana, S.; Kundu, D.J.; Inuganti, A.; Griss, J.; Mayer, G.; Eisenacher, M.; et al. The PRIDE database and related tools and resources in 2019: improving support for quantification data. *Nucleic Acids Res* **2019**, *47*, D442-D450, doi:10.1093/nar/gky1106.